# Molecular mechanism of formation and destruction of a pseudo-capsule in clear cell renal cell carcinoma

TAKUTO SHIMIZU[1], MAKITO MIYAKE[1], KOTA IIDA[1], SAYURI ONISHI[1], TOMOMI FUJII[2], YUSUKE IEMURA[1], KAZUKI ICHIKAWA[1], CHIHIRO OMORI[1], FUMISATO MAESAKA[1], MITSURU TOMIZAWA[1], TATSUKI MIYAMOTO[1], NOBUMICHI TANAKA[3] and KIYOHIDE FUJIMOTO[1]

Departments of [1]Urology, [2]Diagnostic Pathology and [3]Prostate Brachytherapy, Nara Medical University, Kashihara, Nara 634-8522, Japan

Received September 19, 2023; Accepted March 6, 2024

DOI: 10.3892/ol.2024.14358

**Abstract.** The process and molecular mechanisms underlying the formation and destruction of a pseudo-capsule (PC) in clear cell renal cell carcinoma (ccRCC) are poorly understood. In the present study, the PCs of surgical specimens from primary tumors and metastatic lesions in 169 patients with ccRCC, and carcinogen-induced ccRCC rat models were semi-quantified using the invasion of PC (i-Cap) score system. This was based on the relationship among the tumor, PC and adjacent normal tissue (NT) as follows: i-Cap 0, tumor has no PC and does not invade NT; i-Cap 1, tumor has a complete PC and does not invade into the PC; i-Cap 2, tumor with focal absences in the PC, which partially invades the PC but not completely through the PC; i-Cap 3, tumor crosses the PC and invades the NT; i-Cap 4, tumor directly invades the NT without a PC. The study suggested that PC formation was not observed without physical compression, and also revealed that tumor invasion into the PC was a prognostic factor for postoperative oncological outcomes. Higher i-Cap, Fuhrman grade and tumor size were independent poor prognostic factors for postoperative disease-free survival. mRNA expression arrays generated from carcinogen-induced ccRCC rat models were used to explore genes potentially associated with the formation and destruction of a PC. Subsequently, human ccRCC specimens were validated for four genes identified via expression array; the results revealed that collagen type 4A2, matrix metalloproteinase-7 and l-selectin were upregulated alongside the progression of i-Cap score. Conversely, endoglin was downregulated. In conclusion, the present study provides insights into the formation and destruction of a PC, and the results may aid the treatment and management of patients with ccRCC.

*Correspondence to:* Professor Kiyohide Fujimoto, Department of Urology, Nara Medical University, 840 Shijo-cho, Kashihara, Nara 634-8522, Japan
E-mail: kiyokun@naramed-u.ac.jp

*Abbreviations:* PC, pseudo-capsule; RCC, renal cell carcinoma; ccRCC, clear cell RCC; NSS, nephron-sparing surgery; RN, radical nephrectomy; i-Cap, invasion of pseudo-capsule; NT, normal tissue; TNM, Tumor-Node-Metastasis; UICC, Union for International Cancer Control; DEN, N-diethylnitrosamine; FeNTA, ferric nitrilotriacetic acid; H&E, hematoxylin and eosin; IHC, immunohistochemistry; COL4A2, collagen type 4A2; ENG, endoglin; MMP, matrix metalloproteinase; SELL, l-selectin; CSS, cancer-specific survival; DFS, disease-free survival; IQR, interquartile range; HR, hazard ratio; CI, confidence interval; HAI-1, hepatocyte growth factor activator inhibitor type 1; sHAI-1, soluble HAI-1

*Key words:* RCC, PC, prognostic factor, molecular mechanism, rat model

## Introduction

According to the World Health Organization, renal cell carcinoma (RCC) is considered to be the 16th most commonly diagnosed cancer in the world, with RCC-related deaths surpassing 170,000 annually (1). The presence of a pseudo-capsule (PC) in RCC is widely known, and radiographically detectable PC is a distinctive feature in the imaging diagnosis of RCC (2). A PC is located at the border between cancer tissue and normal kidney tissue; therefore, it can be a useful indicator during nephron-sparing surgery (NSS) (3). However, little is currently known about the clinical and biological role of PCs. Pickhardt *et al* (2) suggested that the formation of a PC is derived from tumor growth in an organ, which causes compression and necrosis of the adjacent normal parenchyma resulting in the deposition of fibrous tissue. Wang *et al* (4) reported that the constituent components of a PC in clear cell RCC (ccRCC) include collagen fibers, smooth muscle bundles and some fibroblasts.

PCs have been detected in >90% of RCC cases worldwide, regardless of histopathological subtype, such as clear cell, papillary or chromophobe RCC (5-7). Among these subtypes, ccRCC is most likely to form a thick PC (6,8). By contrast, benign renal neoplasms, such as papillary adenoma and oncocytoma, usually do not have a PC or, if one is present, it tends to be thin (9,10). RCC has the potential of invasion to the PC and, subsequently, to the normal tissues (NTs) beyond the PC. Although RCC invasion to PCs is considered a poor prognostic factor (11,12), a detailed molecular mechanism underlying the

formation and destruction of PCs in RCC has not yet been provided, to the best of our knowledge. The present study investigated the potential mechanisms underlying the formation and destruction of a PC in localized ccRCC using clinical human tissues and a rat model of carcinogenesis.

## Patients and methods

*Inclusion criteria, patient cohort and evaluation of PCs in ccRCC*. The present study was approved by the Institutional Review Board of Nara Medical University (Kashihara, Japan; approval no. NMU-1256) and complied with the 1964 Declaration of Helsinki and its later amendments. All participants provided written informed consent for the present study. Surgical specimens from 169 consecutive patients with localized ccRCC who underwent radical nephrectomy (RN) or NSS with an adequate (≥5 mm) resection margin at the Department of Urology, Nara Medical University Hospital between January 2007 and December 2014 were included in the analysis. The patients did not have any intraoperative capsular damage and did not undergo enucleation. The clinicopathological and follow-up data of the patients were obtained through a retrospective chart review. The extent of the formation and destruction of the PC was evaluated based on the invasion of PC (i-Cap) scoring system (three categories), previously reported by Snarskis *et al* (12). In the present study, a modified i-Cap scoring system was used as follows: i-Cap 0, tumor has no PC and does not invade NT; i-Cap 1, tumor has a complete PC and does not invade into the PC; i-Cap 2, tumor with focal absences in the PC, which partially invades the PC but not completely through the PC; i-Cap 3, tumor crosses the PC and invades the NT; i-Cap 4, tumor directly invades the NT without a PC (Fig. 1). A uropathologist with expertise in RCC pathological diagnosis (FT), blinded to the clinical outcome of the patients, reviewed each hematoxylin & eosin (H&E)-stained specimen. For H&E staining, the specimens were stained with 1.5 g/l hematoxylin for 10 min, washed and then stained with eosin for 2 min at room temperature. Results were observed using a light microscope. Tumors were staged according to the pathological tumor-node-metastasis (TNM) guidelines in the Union for International Cancer Control Staging Manual, 8th edition (13), and were graded according to the criteria set out by the Fuhrman grading system (14). All of the tumors were scored by the i-Cap scoring system, ranging from 0 to 4. The i-Cap classification was heterogeneous within tumors, with the highest values assigned to areas in contact with normal renal tissue (i.e. not areas of the fibrous septum between tumor nodules). Regarding the thickness of the PC, it was also measured at the region with the highest i-Cap score. The thickness of the PC was measured and the mean of two observer results was taken using scan images from a fluorescence microscope (EVOS FL Auto, AMAFD1000; Thermo Fisher Scientific, Inc.) (Fig. 1).

*Evaluation of PC formation of metastatic lesions*. Out of the 169 patients, a total of 15 specimens of metastatic lesions from 14 patients who underwent metastasectomy for metastatic ccRCC were evaluated for i-Cap and PC formation. Surgical resection of metastases aimed to reduce the cancer burden, control pain or prevent paralysis.

*Identification of genes involved in PC destruction with ccRCC rat models*

*N-diethylnitrosamine (DEN)-initiated and ferric nitrilotriacetate (FeNTA)-promoted rat models of ccRCC*. An *in vivo* rat carcinogenic model of ccRCC was created via intraperitoneal administration of DEN and FeNTA (both Tokyo Chemical Industry Co., Ltd.) according to reports by Toyokuni *et al* (15) and Vargas *et al* (16). A total of 32 female Wistar rats (age, 2 weeks) were purchased from Oriental Bio Service Ltd. The experiment started from 4 weeks after birth, and the mean weight at the beginning of the experiment was 110 g (range, 98-130 g). All animal studies were approved by the institutional animal care and use committee of Nara Medical University and were conducted in accordance with local humane animal care standards (approval no. 12211). This animal study was conducted at Nara Medical University between February and September 2019. Animal care was conducted in compliance with the recommendations of The Guide for Care and Use of Laboratory Animals (National Research Council) (17). All rats were maintained under pathogen-free conditions, were provided with free access to sterile food and water, and were kept under controlled, stable ambient conditions (23±3˚C; 12-h light/dark cycle; 50±20% humidity). The dietary intake and body weight of rats were monitored every week, and termination of the experiment was considered if the rats refused food and significant weight loss was observed. Rats were also visually inspected daily to check whether the tumor was large enough to be visible on the body surface or whether the rats were exhibiting significant ascites. If these conditions were suspected, euthanasia was considered. During the experiment, if the orthotopic tumor grew to a size where it could be seen from the body surface, or weight loss of ≥20% occurred within 2 to 3 days or weight loss of ≥25% occurred within 7 days, euthanasia was performed. The greatest weight loss observed was 16 g (from 498 to 482 g) in 1 week.

The control group and ccRCC model group of 12 and 20 rats were prepared, respectively. In the ccRCC model group, DEN was administered intraperitoneally at a dose of 200 mg/kg, followed by intraperitoneal administration of FeNTA at a dose of 9 mg/kg twice a week for 12, 16, 20 and 24 weeks. All rats were euthanized by cervical dislocation under anesthesia with isoflurane (induction 4%, maintenance 2-3%) 8 weeks after the complete administration of carcinogens. The control group also underwent euthanasia at the same time and in the same manner as the test group. Subsequently, the kidneys were removed, placed on filter paper and fixed in 10% neutral buffered formalin for 18 h at room temperature. The paraffin-embedded tissues were cut into 5-$\mu$m pieces and subjected to H&E staining on glass slides. For H&E staining, the specimens were stained with 1.5 g/l hematoxylin for 10 min, washed and then stained with eosin for 2 min at room temperature. The results were then observed using a light microscope. The step-sections of the kidneys were observed under a light microscope, and the relationship between the PC and the tumor was investigated. The kidneys were fixed in formalin immediately after removal so that the gap between the tumor and normal kidney tissue could be observed; therefore, only the tumor was removed and the tumor size and weight were not measured. Evaluation of i-Cap in rat models was also performed by the same pathologist (FT) that evaluated

| i-Cap | Representative Image (H&E ×100 ) | Description |
|---|---|---|
| i-Cap 0 | 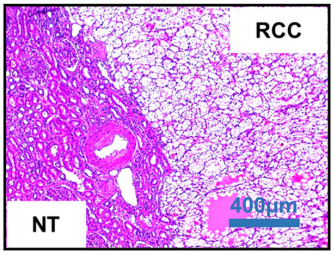 | Tumor has no PC and does not invade into NT |
| i-Cap 1 | 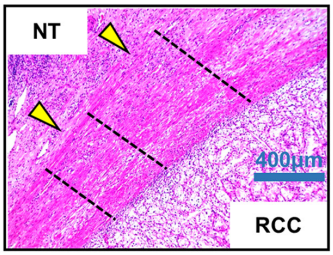 | Tumor with complete PC and does not invade into PC |
| i-Cap 2 | 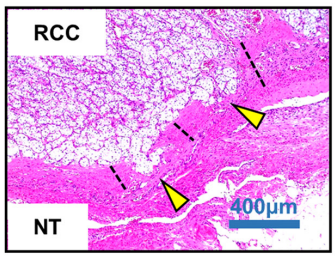 | Tumor with focal absences in PC that invade partially into and yet not completely through PC |
| i-Cap 3 | 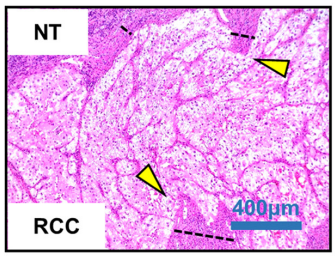 | Tumor crosses PC and invades NT |
| i-Cap 4 | 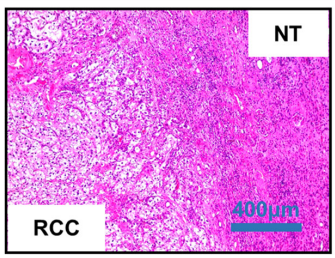 | Tumor directly invades NT without PC |

Figure 1. i-Cap scoring system. Representative images of i-Cap 0, 1, 2, 3 and 4 are shown (x100 magnification). Yellow arrows show PCs; black dotted lines indicate PC thickness. Scale bar, 400 $\mu$m. RCC, renal cell carcinoma; H&E, hematoxylin and eosin; NT, normal tissue; PC, pseudo-capsule; i-Cap, invasion of PC.

the human specimens. The lungs and livers were also removed and treated in the same way as the kidneys to assess whether tumors were present outside of the kidneys, but no metastatic tumors were identified.

*Identification of genes involved in PC destruction*. Reverse transcription-quantitative PCR (RT-qPCR) was performed to measure the expression levels of mRNA. Total RNA was extracted using a miRNeasy FFPE kit (Qiagen GmbH), according to the manufacturer's instructions. Conversion to cDNA was performed using an RT2 First Standard kit (Qiagen GmbH), according to the manufacturer's instructions. cDNA was added to RT$^2$ SYBR Green qPCR Mastermix (Qiagen GmbH) and the mRNA expression of ~400 genes was measured using three RT$^2$ Profiler PCR Array panels as follows: Rat Extracellular Matrix & Adhesion Molecules (cat. no. PARN-013ZD), Rat Tumor Metastasis (cat. no. PARN-028ZD) and Rat Fibrosis (cat. no. PARN-120ZD) (all from Qiagen GmbH) in NT around the PC and tumor tissue around the PC to identify genes that were upregulated or downregulated in the formation and destruction of the PC.

RT-qPCR and Heat map analysis were performed using the CFX96 Touch Real-Time PCR Detection System (Bio-Rad Laboratories, Inc.), in a manner similar to that reported in our previous study (18). RT-qPCR was performed under the following conditions: Denaturation at 95˚C for 10 min; 40 cycles of denaturation at 95˚C for 15 sec; and annealing and extension at 60˚C for 1 min. Primer sequences were not available due to trade secrets. mRNA expression was compared between the i-Cap 1 group and the i-Cap 2-3 group. Relative expression was normalized to Actb, B2m, Hprt1, Ldha and Rplp1 expression, as the use of multiple housekeeping genes is known to increase reliability (19), and estimated using the $2^{-\Delta\Delta Cq}$ method (20). Results were presented as the fold-change relative to the control.

*Confirmation of the relevant gene groups in human ccRCC specimens via immunohistochemistry (IHC)*. IHC was used to assess whether the genes identified in the rat model were involved in PC formation and destruction in human ccRCC specimens. Resected tissue specimens were fixed in 10% formalin, incubated overnight at room temperature and embedded in paraffin. Paraffin-embedded blocks were then cut into 3-$\mu$m sections and placed on Superfrost Plus microslides (Thermo Fisher Scientific, Inc.). Sections were deparaffinized in xylene and hydrated in decreasing concentrations of ethyl alcohol, and antigen retrieval was carried out via autoclaving with citric acid buffer (pH 6.0) for 20 min at 120˚C. Next, the sections were incubated with 3% hydrogen peroxide for 15 min at room temperature to block endogenous peroxidase activity. IHC staining was performed using the Histofine SAB-PO (Multi) kit (cat. no. 424043; Nichirei Biosciences, Inc.) according to the manufacturer's instructions. Non-specific binding was blocked by incubating the sections with 10% normal goat serum for 10 min. The sections were incubated with monoclonal antibodies against collagen type 4A2 (COL4A2; cat. no. ab125208; 1:500 dilution; Abcam), matrix metalloproteinase-7 (MMP-7; cat. no. MAB9071; 1:200 dilution; R&D Systems, Inc.), endoglin (ENG; cat. no. AF1097; 1:100 dilution; R&D Systems, Inc.) and l-selectin (SELL; cat. no. sc-390756; 1:50 dilution; Santa Cruz Biotechnology, Inc.) overnight at 4˚C. The secondary antibody reaction was performed using Histofine SAB-PO (Multi) kit (cat. no. 424043, Nichirei Biosciences, Inc.) according to the manufacturer's instructions. The slides were developed with DAB (Histofine, cat. no. 415172, Nichirei Biosciences, Inc.) until the signal clearly appeared, and the nuclei were stained with Mayer's hematoxylin for 1 min at room temperature, dehydrated and sealed with a cover slip. Images were obtained using a fluorescence microscope (EVOS FL Auto, AMAFD1000; Thermo Fisher Scientific, Inc.). All stained tissue samples were evaluated by two investigators (YI and TM) without knowledge of the patient data. The tumor tissues and NTs around the PC from the region in which the i-Cap score was assigned were evaluated by immunostaining.

The sections were analyzed and staining was assessed using a semiquantitative grading system based on a previous report by Allred *et al* (21). Briefly, the expression level of each marker was scored by assigning a proportion score and an intensity score. The proportion score represents the estimated proportion of immunoreactive cells or stroma: 0, 0% of cells; 1, 0-1%; 2, 1-10%; 3, 10-33%; 4, 33-67%; 5, 67-100%. The intensity score represents the average intensity of positive cells or stroma: 0, none; 1, weak; 2, intermediate; 3, strong. The proportion and intensity scores were added to obtain a combined immunostaining score for the expression of each marker, which ranged from 0 to 8: 0, none; 1-2, low; 3-4, moderate; 5-6, high.

*Statistical analysis*. Statistical analyses were performed using GraphPad Prism 5.0 (Dotmatics). The associations between i-Cap and tumor clinicopathological variables or IHC results were evaluated by Kruskal-Wallis test and the Dunn's multiple comparison test or Fisher's exact test. Cancer-specific survival (CSS) or disease-free survival (DFS) were estimated using the Kaplan-Meier method. CSS endpoints were defined as death due to RCC after surgery. DFS endpoints were defined as distant metastasis, local recurrence or death from any cause after surgery. CSS or DFS were calculated from the day when nephrectomy or NSS was performed until the last follow-up or death by RCC, or when RCC recurrence or metastasis were diagnosed. The differences between each group were compared using the log-rank test. Multivariate logistic and Cox regression analyses were performed using SPSS software version 21 (IBM Corp.) to identify factors that predict postoperative DFS and CSS. All tests were two-sided and $P<0.05$ was considered to indicate a statistically significant difference.

## Results

*Relationship between PCs and clinicopathological characteristics in ccRCC*. Table I shows the clinicopathological information of 169 patients who underwent surgery at Nara Medical University between 2007 and 2014. The median follow-up period was 91 months (interquartile range, 60-114 months). During the follow-up period, 39 patients (23.1%) experienced metastasis and 4 patients (2.4%) had local recurrence. Among them, 1 patient showed both local recurrence and metastasis. A total of 33 patients (19.5%) died; of these, 16 (9.5%) died due to ccRCC. Table I also summarizes the relationship between i-Cap and PC thickness, tumor size and Fuhrman grade. Patients with i-Cap 3 had a significantly thinner PC than those with i-Cap 1. Notably, there was no significant difference between i-Cap 2 and i-Cap 1. In addition, patients with i-Cap 2, 3 and 4 had significantly larger tumor diameters than those with i-Cap 1. In addition, patients with i-Cap 3 and 4 had a higher proportion of high Fuhrman grades than those with i-Cap 1.

*Prognostic factors after surgery*. The Kaplan-Meier curves for DFS and CSS based on i-Cap score are displayed in Fig. 2. CSS and DFS were lower as the i-Cap score increased (Fig. 2A and B). Patients with PC invasion (i-Cap 2-4) had significantly worse DFS and CSS compared with those without PC invasion (i-Cap 0 and 1) [hazard ratio (HR) 4.13, 95% confidence interval (CI) 2.27-7.67, $P<0.001$; HR 6.16, 95% CI 2.29-16.6, $P<0.001$] (Fig. 2C and D). Multivariate analysis revealed that i-Cap, Fuhrman grade and tumor size were negative prognostic factors for DFS, and i-Cap and tumor size were negative prognostic factors for CSS (Table II).

Table I. Clinicopathological information of patients in each i-Cap score group.

| Variable | Total | i-Cap 0 | i-Cap 1 | i-Cap 2 | i-Cap 3 | i-Cap 4 |
|---|---|---|---|---|---|---|
| Cases, n | 169 | 5 | 89 | 41 | 25 | 9 |
| Age, years | | | | | | |
| Median (IQR) | 64 (56-74) | 73 (71-75) | 65 (53-73) | 67 (56-74) | 67 (62-74) | 63 (62-64) |
| Sex, n | | | | | | |
| Male | 126 | 3 | 67 | 39 | 19 | 8 |
| Female | 43 | 2 | 22 | 2 | 6 | 1 |
| Sugery, n | | | | | | |
| RN | 134 | 2 | 60 | 41 | 22 | 9 |
| NSS | 35 | 3 | 29 | 0 | 3 | 0 |
| Tumor size, mm | | | | | | |
| Median (IQR) | 45.0 (26.0-65.0) | 23.5 (16.5-32.8) | 34.0 (20.0-50.8) | 48.0 (36.5-60.0) | 64.0 (45.8-100.5) | 60 (51.5-120) |
| P-value | | ns | Ref[a] | <0.05[a] | <0.001[a] | <0.01[a] |
| Serum CRP, mg/l | | | | | | |
| Median (IQR) | 0.1 (0.1-0.3) | 0.1 (0.1-0.4) | 0.1 (0.1-0.3) | 0.1 (0.0-0.2) | 0.1 (0.1-1.1) | 1.3 (0.1-4.6) |
| Serum Alb, g/dl | | | | | | |
| Median (IQR) | 4.3 (4.0-4.6) | 4.6 (4.5-4.6) | 4.3 (4.0-4.5) | 4.3 (4.1-4.7) | 4.2 (4.0-4.5) | 4.0 (4.0-4.4) |
| Pathological T stage, n | | | | | | |
| 1 | 99 | 2 | 65 | 25 | 6 | 1 |
| 2 | 6 | 0 | 4 | 1 | 1 | 0 |
| 3 | 61 | 3 | 18 | 15 | 18 | 7 |
| 4 | 3 | 0 | 2 | 0 | 0 | 1 |
| INF, n | | | | | | |
| a | 77 | 4 | 59 | 11 | 1 | 2 |
| b and c | 92 | 1 | 30 | 30 | 24 | 7 |
| PC thickness, mm | | | | | | |
| Median (IQR) | 0.62 (0.36-1.02) | | 0.72 (0.39-1.26) | 0.57 (0.42-0.71) | 0.37 (0.25-0.70) | |
| Mean ± SD | 0.74±0.49 | | 0.85±0.55 | 0.69±0.39 | 0.49±0.31 | |
| P-value | | NA | Ref[a] | ns[a] | <0.05[a] | NA |
| Fuhrman grade maximum, n | | | | | | |
| 1 and 2 | 122 | 5 | 72 | 31 | 12 | 2 |
| 3 and 4 | 47 | 0 | 17 | 10 | 13 | 7 |
| P-value | | 0.58[b] | Ref[b] | 0.49[b] | <0.01[b] | <0.01[b] |
| Disease recurrence after surgery, n | | | | | | |
| Distant metastasis | 39 | 0 | 10 | 12 | 12 | 5 |
| Local recurrence | 4 | 0 | 1 | 0 | 1 | 2 |
| Follow-up, months | | | | | | |
| Median (IQR) | 91 (60-114) | 105 (68-107) | 93 (63-114) | 85 (68-127) | 95 (62-117) | 49 (15-84) |

IQR, interquartile range; RN, radical nephrectomy; NSS, nephron-sparing surgery; i-Cap, invasion of pseudo-capsule; Ref, reference (compared with the other groups); NA, not analyzed; SD, standard deviation; CRP, C-reactive protein; Alb, albumin; INF, infiltration. [a]Kruskal-Wallis test and Dunn's multiple comparisons test; [b]Fisher's exact test.

*Evaluation of PC formation in each metastatic lesion*. The present study evaluated 15 specimens from 14 patients who underwent resection of metastatic ccRCC at Nara Medical University. The 15 specimens consisted of 6 from the lung, 3 from skeletal muscle and bone, and 1 from the skin, contralateral kidney and fat (adipose tissue in the abdomen). As shown in Fig. 3, in all cases, PC formation was observed in the primary kidney tumor, although there was a difference

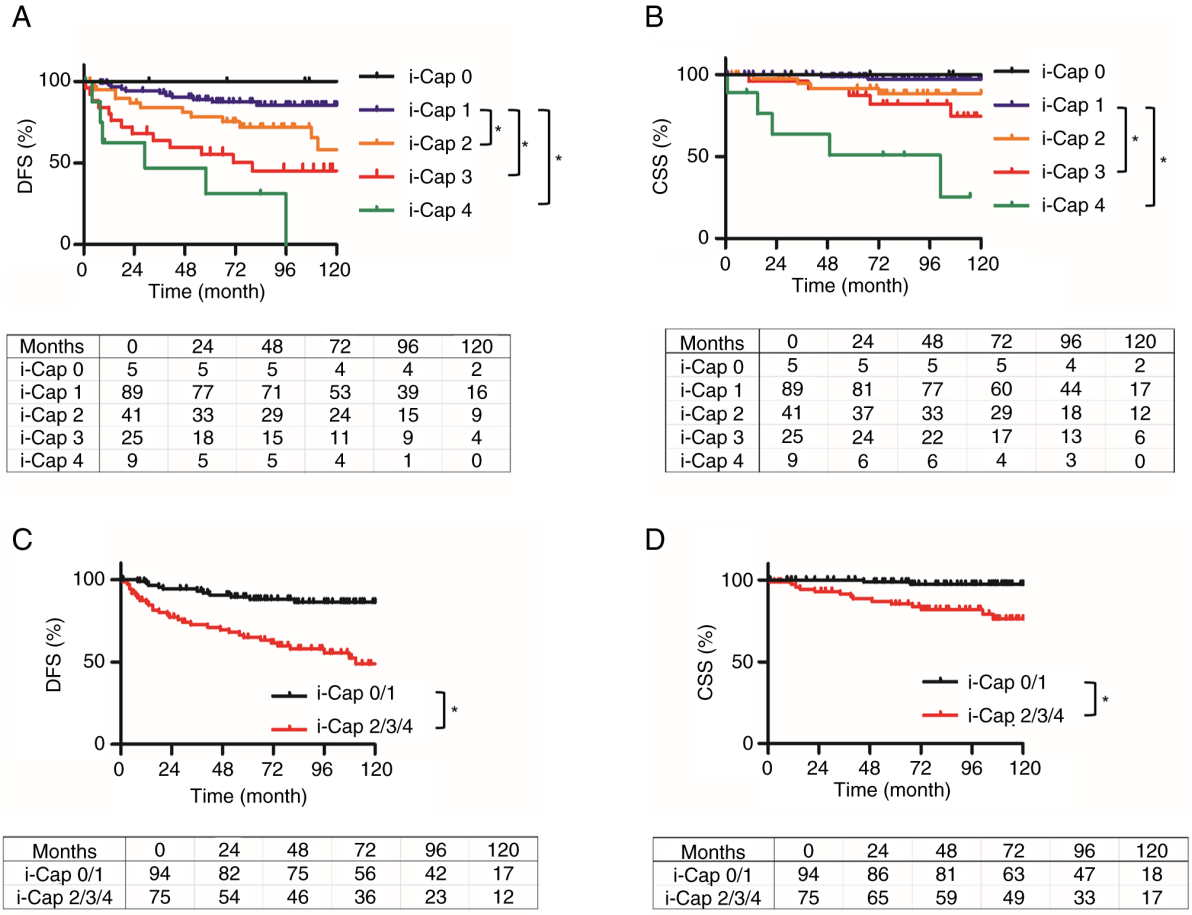


| Months | 0 | 24 | 48 | 72 | 96 | 120 |
|---|---|---|---|---|---|---|
| i-Cap 0 | 5 | 5 | 5 | 4 | 4 | 2 |
| i-Cap 1 | 89 | 77 | 71 | 53 | 39 | 16 |
| i-Cap 2 | 41 | 33 | 29 | 24 | 15 | 9 |
| i-Cap 3 | 25 | 18 | 15 | 11 | 9 | 4 |
| i-Cap 4 | 9 | 5 | 5 | 4 | 1 | 0 |

| Months | 0 | 24 | 48 | 72 | 96 | 120 |
|---|---|---|---|---|---|---|
| i-Cap 0 | 5 | 5 | 5 | 5 | 4 | 2 |
| i-Cap 1 | 89 | 81 | 77 | 60 | 44 | 17 |
| i-Cap 2 | 41 | 37 | 33 | 29 | 18 | 12 |
| i-Cap 3 | 25 | 24 | 22 | 17 | 13 | 6 |
| i-Cap 4 | 9 | 6 | 6 | 4 | 3 | 0 |

| Months | 0 | 24 | 48 | 72 | 96 | 120 |
|---|---|---|---|---|---|---|
| i-Cap 0/1 | 94 | 82 | 75 | 56 | 42 | 17 |
| i-Cap 2/3/4 | 75 | 54 | 46 | 36 | 23 | 12 |

| Months | 0 | 24 | 48 | 72 | 96 | 120 |
|---|---|---|---|---|---|---|
| i-Cap 0/1 | 94 | 86 | 81 | 63 | 47 | 18 |
| i-Cap 2/3/4 | 75 | 65 | 59 | 49 | 33 | 17 |

Figure 2. Kaplan-Meier curves of DFS and CSS for each i-Cap score, and for patients with or without invasion of the PC. DFS and CSS were estimated using the Kaplan-Meier method. (A) DFS of patients in each i-Cap group. Compared with in patients with i-Cap 1, those with i-Cap 2, 3 and 4 had a significantly worse DFS. (B) CSS of patients in each i-Cap group. Compared with in patients with i-Cap 1, those with i-Cap 3 and 4 had a significantly worse CSS. (C) DFS was compared between two groups, those which exhibited invasion into the PC or normal renal tissue (i-Cap 2/3/4) and those that did not (i-Cap 0/1). Compared with in patients with i-Cap 0/1, those with i-Cap 2/3/4 had a significantly worse DFS. (D) CSS compared between two groups, those which exhibited invasion into the PC or normal renal tissue (i-Cap 2/3/4) and those that did not (i-Cap 0/1). Compared with in patients with i-Cap 0/1, those with i-Cap 2/3/4 had a significantly worse CSS. *P<0.05. DFS, disease-free survival; CSS, cancer-specific survival; PC, pseudo-capsule; i-Cap, invasion of PC.

in the i-Cap score. In addition, there was a difference in PC formation depending on the metastatic site. Specifically, PC formation was not observed in organs that are considered to lack an epithelial component and have a lower elastic modulus than that of the kidney (22,23).

*Identification of genes involved in PC formation and destruction in ccRCC rat models*. A total of 3 rats from the control group and 5 rats from the ccRCC rat model group were sacrificed at each time point 8 weeks after the end of FeNTA administration. Macroscopic images of kidneys from rats with ccRCC at each time point of FeNTA administration (12, 16, 20 and 24 weeks) showed a tendency for renal tumors to grow with multiple occurrences (Fig. 4A). Microscopic images of renal tumors at each time point of FeNTA administration exhibited a trend towards an increase in i-Cap score as the administration period increased (Fig. 4B).

Heat map analysis compared mRNA expression levels between rats with ccRCC in the i-Cap 1 and i-Cap 2-3 groups (Fig. 5A). The areas shown in red are upregulated, and the areas shown in green are downregulated. Also, the areas displayed in black are not regulated. Black text with a white cross indicates that there is no calculated value. The present study paid attention to the extracellular matrix, angiogenesis and immune-related markers among the genes that had a difference of >2-fold in RT-qPCR results. The expression levels of *COL4A2*, *ENG*, *MMP-7* and *SELL* were enhanced in the i-Cap 2-3 group compared with those in the i-Cap 1 group, with a >2-fold difference.

*Evaluation of four genes identified in a rat model of ccRCC in human specimens*. The semi-quantified scores are shown in Fig. 5B. Representative IHC images of COL4A2, MMP-7, ENG and SELL immunostaining for each i-Cap score are shown (Fig. 5C). For COL4A2, MMP-7 and SELL, it was indicated that the expression levels of these proteins increased as i-Cap progressed, that is, as PC destruction progressed. By contrast, the opposite was true for ENG, indicating that protein expression decreased as i-Cap progressed.

## Discussion

The present study investigated the processes involved in the formation and destruction of a PC in ccRCC. To the best of our

Table II. Multivariate analysis for DFS and CSS.

| | DFS | | | CSS | | |
|---|---|---|---|---|---|---|
| | Multivariate analysis | | | Multivariate analysis | | |
| Variable | HR | 95% CI | P-value | HR | 95% CI | P-value |
| UICC 8th pT stage (pT1/2/3/4)[a] | 1.05 | 0.69-1.59 | 0.82 | 1.09 | 0.49-2.41 | 0.84 |
| Fuhrman grade (G1-4)[a] | 1.95 | 1.17-3.25 | 0.010 | 1.44 | 0.65-3.23 | 0.37 |
| Size (mm)[b] | 1.02 | 1.00-1.27 | 0.010 | 1.02 | 1.00-1.04 | 0.02 |
| INF (a/b/c)[a] | 1.34 | 0.64-2.78 | 0.44 | 1.19 | 0.29-4.87 | 0.81 |
| Serum CRP (mg/l)[b] | 0.95 | 0.86-1.06 | 0.39 | 1.00 | 0.85-1.17 | 0.39 |
| Serum Alb (g/dl)[b] | 0.80 | 0.39-1.66 | 0.55 | 0.60 | 0.85-1.17 | 0.55 |
| i-Cap (0-4)[a] | 1.60 | 1.13-2.25 | <0.01 | 2.20 | 1.20-4.01 | 0.01 |

DFS, disease-free survival; CSS, cancer-specific survival; HR, hazard ratio; CI, confidence interval; UICC Union for International Cancer Control; pT, pathological tumor; INF, infiltration; CRP, C-reactive protein; Alb, albumin; i-Cap, invasion of pseudo-capsule. [a]Ordinal variable; [b]continuous variable.

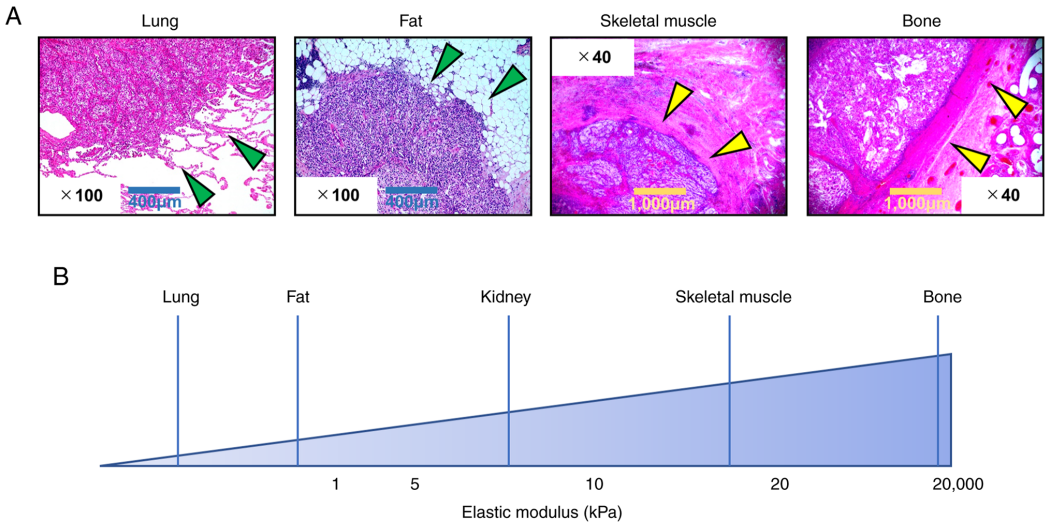


C

| | Renal lesion | | Metastasectomy 1 | | Metastasectomy 2 | |
|---|---|---|---|---|---|---|
| | i-Cap | PC formation | Site | PC formation | Site | PC formation |
| Case 1 | 1 | + | Lung | − | Skeletal muscle | + |
| Case 2 | 1 | + | Lung | − | | |
| Case 3 | 2 | + | Lung | − | | |
| Case 4 | 2 | + | Lung | − | | |
| Case 5 | 3 | + | Lung | − | | |
| Case 6 | 1 | + | Lung | − | | |
| Case 7 | 1 | + | Fat | − | | |
| Case 8 | 3 | + | Contralateral kidney | + | | |
| Case 9 | 1 | + | Skeletal muscle | + | | |
| Case 10 | 1 | + | Skeletal muscle | + | | |
| Case 11 | 1 | + | Skin | + | | |
| Case 12 | 1 | + | Bone | + | | |
| Case 13 | 2 | + | Bone | + | | |
| Case 14 | 2 | + | Bone | + | | |

Figure 3. Evaluation of PCs in each metastatic site. (A) Representative images of metastasis (x40 and x100 magnification). Yellow arrows indicate PC formation and green arrows indicate no PC formation. Scale bars, 400 or 1,000 $\mu$m. Although PC formation was not observed in fat and lung tissues, it was observed in muscle and bone. (B) Schematic diagram showing the elastic modulus of the kidney and each organ based on the reports by Butcher *et al* (16) and Handorf *et al* (17). (C) Table showing the presence or absence of PC formation in primary renal tumors and resected metastatic lesions. PC, pseudo-capsule; i-Cap, invasion of PC.

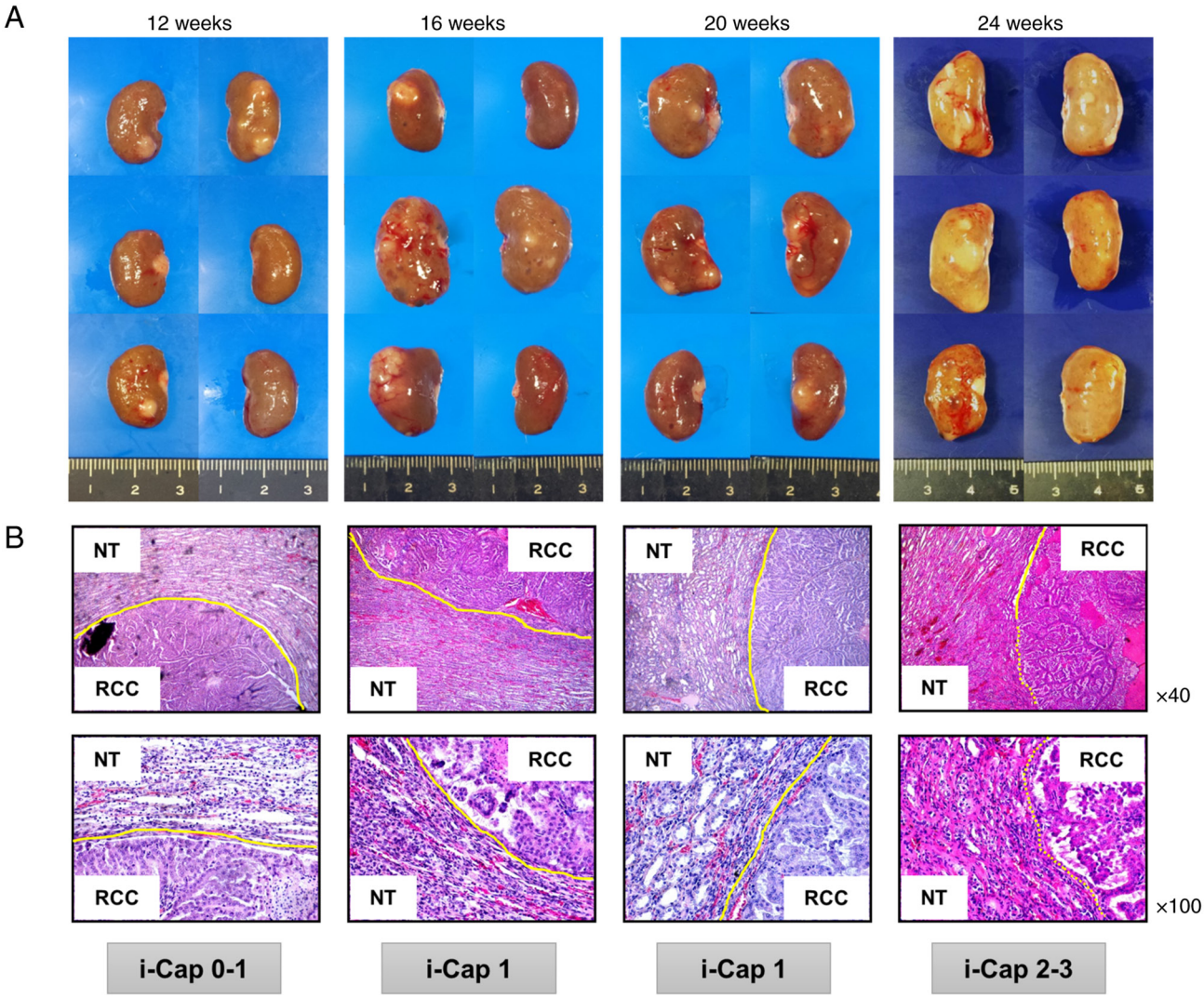


Figure 4. Macroscopic and microscopic images of kidneys of a rat model of ccRCC. Representative (A) macroscopic and (B) microscopic images of the rat models (x40 and x100 magnification). As the administration period of ferric nitrilotriacetic acid and N-diethylnitrosamine increased, the number and size of tumors tended to increase, and a corresponding exacerbation of i-Cap score was observed. The solid yellow line indicates the formation of a PC; the dotted yellow line shows the broken part of the PC. ccRCC, clear cell renal cell carcinoma; NT, normal tissue; PC, pseudo-capsule; i-Cap, invasion of PC.

knowledge, no similar study has yet been published. Firstly, the present study confirmed the presence of tumors in which a PC was not formed in local ccRCC, and these tumors were classified as i-Cap 0. Only 5 out of 169 cases (3%) were classified as i-Cap 0, with smaller tumor size and lower Fuhrman grade compared with the others. Additionally, in the evaluation of metastatic lesions, PC formation was observed in the primary tumor site (i.e. the kidney) in all cases; however, although this information was only available from a sample size of 14 cases, no evidence of PC formation in soft tissues, such as fat and lungs, which are known to have low elastic moduli, was identified. Evaluation of the elastic modulus of each tissue by Butcher *et al* (22) and Handorf *et al* (23) reported that fat and lung tissues are less stiff than the kidney, whereas muscle and bone are stiffer than the kidney. A plausible hypothesis derived from the present metastasectomy findings is that a PC does not form in ccRCC when normal tissue stiffness is lower than that of tumors, especially when the epithelial component is absent. In addition, i-Cap 0 tumors were characterized by very small diameters and low-grade tumors. Previous research has indicated that low-grade ccRCC tumors exhibit a significantly slower growth rate compared with high-grade ccRCC tumors (24,25). This suggests that i-Cap 0 tumors may also possess a very slow growth rate. Given their small size and slow proliferation, it is possible that the normal renal parenchyma is not compressed, leading to the absence of PC formation. Evaluation of PC formation in these metastases and the pathological features of i-Cap 0 tumors indicated that a PC is caused by the physical exclusion of normal parenchymal components, as reported by Pickhardt *et al* (2).

The present study also focused on the destruction of PCs and used the i-Cap classification reported by Snarskis *et al* (12) as a reference. The difference between this previous study and the present study is that the current study used the classification i-Cap 0 when there was no PC formation, whereas the i-Cap classification was the same as Snarskis *et al* when a PC was present. The present study examined the relationship between PC thickness, tumor size and Fuhrman grade for each i-Cap group. As the i-Cap score increased, the PC became thinner, the tumor diameter became larger and the degree

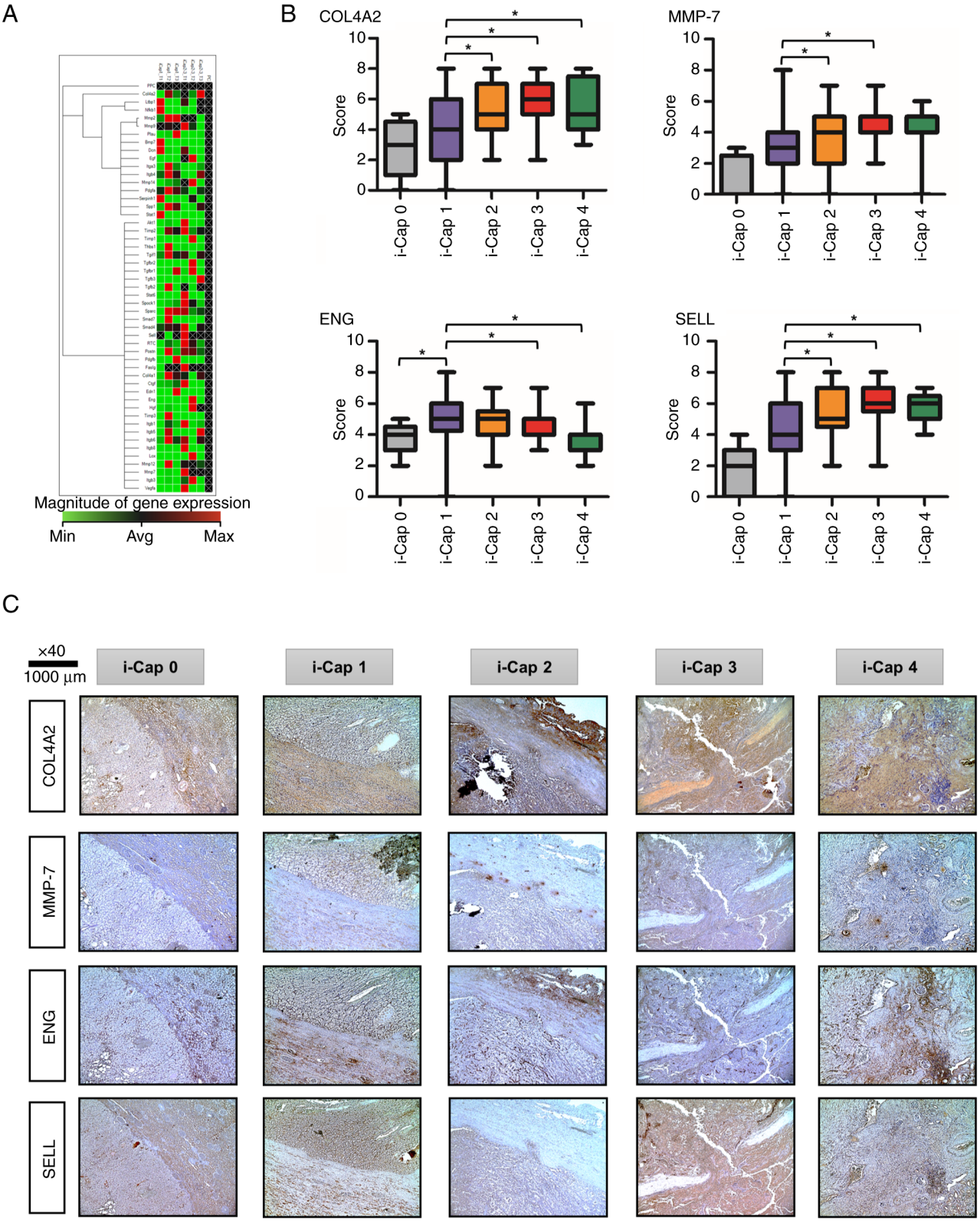


Figure 5. Factors associated with i-Cap score, and their immunohistochemical staining and score comparison. (A) Heat map demonstrating the differences in mRNA expression levels between the i-Cap 1 and i-Cap 2/3 groups in a rat model of ccRCC, as revealed through PCR panel analysis. (B) Immunostaining scores of each protein in each i-Cap score group. *P<0.05 (Kruskal-Wallis and Dunn's post hoc test). (C) Representative images of immunohistochemical staining of human specimens for four proteins in each i-Cap score group (x40 magnification). COL4A2, collagen type 4A2; MMP-7, matrix metalloproteinase-7; ENG, endoglin; SELL, l-selectin; i-Cap, invasion of psuedo-capsule; min, minimum; avg, average; max, maximum.

of malignancy also increased. In addition, the i-Cap score also increased as tumors became more aggressive. Notably, i-Cap was associated with oncological prognosis according to the results of a univariate analysis, and i-Cap and tumor size were identified as prognostic factors for both DFS and CSS in multivariate analyses in the present study. The present

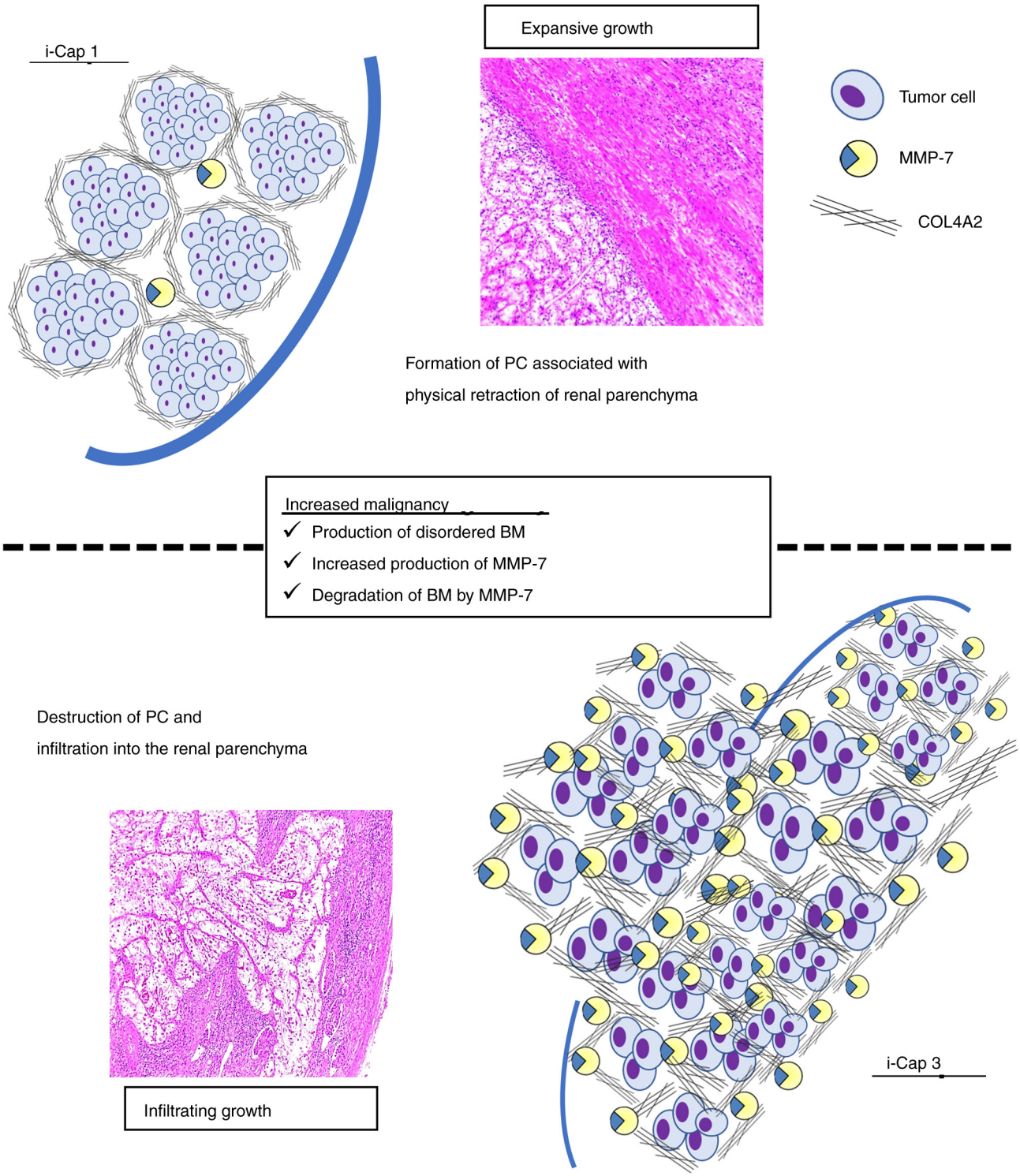


Figure 6. Schematic diagram comparing i-Cap 1 and i-Cap 3. i-Cap 1 shows increased extensibility and PC formation due to physical retraction. The expression of MMP-7 is low, and the disturbance of the BM structure by COL4A2 is also modest. i-Cap 3 shows increased invasiveness, breaking through the PC and invading the renal parenchyma. It shows an increase in MMP-7 expression and disruption of the alliance of the BM structure by COL4A2. PC, pseudo-capsule; COL4A2, collagen type 4A2; MMP-7, matrix metalloproteinase-7; BM, basement membrane.

finding that PC invasion is a factor of poor oncological prognosis is consistent with the findings of Cho *et al* (11). In the present study, only 4 of 169 patients had local recurrence. Of these, only 1 patient was treated with NSS; this patient was 1 of 29 classified as i-Cap 1 and 1 out of 35 who underwent NSS. None of the 3 patients who underwent NSS and were classified as i-Cap 3 experienced local recurrence. Therefore, it was difficult to assess the association between NSS, i-Cap and local recurrence in the present study.

In the FeNTA-administered ccRCC rat model, it was confirmed that the tumors occurred more frequently and growth increased as the administration period progressed. In addition, the tendency of a PC to collapse with the extension of the administration period was confirmed. This suggests that

the destruction of a PC is caused by tumor growth and exacerbation. To identify the molecules involved in PC destruction, comprehensive RNA analysis was performed using tumors obtained from rats with ccRCC from the i-Cap 2-3 and i-Cap 1 groups. As a result, the present study paid attention to the extracellular matrix, angiogenesis and immune-related markers, which had a fold difference of >2. Subsequently, immunohistochemical staining was performed for the PC destruction-associated molecules in the tumor margin of human localized RCC specimens and their expression was evaluated in each i-Cap group.

COL4 is a major component of the basement membrane (BM) in the extracellular matrix. In renal tumors, COL4A1 and COL4A2 chains have been detected in the BM (26). Disturbance of BM structure and an increase in density are seen with increasing malignancy in RCC (27). Furthermore, Provenzano *et al* (28) showed that collagen rearrangement and densification in breast cancer can promote tumorigenesis and invasion into surrounding tissues. These findings support the present finding that the expression of COL4 is enhanced with exacerbation of i-Cap.

MMP-7 is a member of the MMP family of extracellular matrix-degrading enzymes. It is well known that MMPs are upregulated in various types of cancer, and play important roles in cancer invasion and metastasis (29-31). Among them, MMP-7 is considered to be produced primarily by fibroblasts, inflammatory cells and cancer cells, and to degrade proteoglycans, elastin, COL4 and fibronectin (32). MMP-7 has been shown to be enhanced at the invasion front of malignant tumors of esophageal squamous cell carcinoma (29) and colorectal carcinoma (31), indicating a direct role in cancer cell invasion. In addition, in RCC, Miyata *et al* (30) reported enhanced expression at the invasion tip. In the present study of PC rupture, MMP-7 expression increased in response to PC destruction, suggesting that MMP-7 serves a role in RCC peri-invasion. Fig. 6 schematically shows the differences in extracellular matrix reconstruction by COL4 and MMP-7 between i-Cap 1 and 3. MMP-7 cleaves the cancer cell membrane protein hepatocyte growth factor activator inhibitor type 1 (HAI-1) to produce a soluble HAI-1 (sHAI-1) fragment. It has been shown that sHAI-1 and MMP-7 cooperate to induce cancer cell aggregation and metastasis, and therapeutics targeting sHAI-1 have attracted attention (33). Although the current study did not detect sHAI-1 expression, it was confirmed that expression of MMP-7 at the site of invasion was high, which may benefit from sHAI-1-targeted therapy.

RCC is known to be hypervascular and rich in neovascularization, but is also a highly heterogeneous tumor. Unsupervised transcriptome analysis of 823 tumors from patients with advanced RCC by Motzer *et al* (34) revealed that the combination of angiogenesis, immunity, cell cycle, metabolism and stromal programs are classified into seven distinct molecular subsets. Tyrosine kinase inhibitors are effective in subsets with high angiogenesis, and immune checkpoint inhibitors improve clinical benefit in tumors with high T effector and/or cell cycle transcription. These subset classifications were performed for each international metastatic RCC database consortium risk classification used to classify the prognosis of metastatic renal cancer, and it was shown that the classification of the immune system subset gradually increases and that of the angiogenic system subset gradually decreases while exacerbating from favorable risk to intermediate and poor risk. Ohe *et al* (35) and Cioca *et al* (36) also showed that decreased blood vessel density in RCC is associated with exacerbation of cancer malignancy. The present finding that higher i-Cap was associated with a poorer prognosis and decreased ENG expression is consistent with these findings.

SELL is a cell adhesion molecule involved in lymphocyte migration, which is expressed on most circulating leukocytes. Notably, loss of SELL is indicative of T-cell activation as it occurs upon cell activation. ccRCC has been characterized as having one of the highest immune infiltration scores in pan-cancer analyses (37,38). In recent years, the immunoscore has attracted attention in the field of colon cancer, as it reflects the oncological prognosis. The immunoscore ranges from I0, the so-called 'cold' tumor (no or low density of immune cells both at the periphery and center of the tumor), to I4, the so-called 'hot' tumor (high immune cell density at both the periphery and center of the tumor), and is used to classify cancer according to immune infiltration (39). Page *et al* (40) also reported that the infiltration of immune cells at the infiltration site of the tumor margin is related to prognosis. Notably, ccRCC is considered to have a poor prognosis as immune cell infiltration increases (41). In the present study, the expression of SELL was detected, focusing on the infiltration of PC. As a result, it was confirmed that the expression of SELL was enhanced as the i-Cap score increased. This suggests the possibility that immune cell infiltration occurs along with PC destruction.

As aforementioned, it has been confirmed that tumor infiltration into the PC, which is associated with exacerbation of tumor malignancy, is accompanied by decreased angiogenesis, destruction of the extracellular matrix by MMP-7 and reconstruction by COL4, and infiltration of immune cells. This finding may be the key to identifying the PC features that accompany most cases of ccRCC.

The present study has various limitations. First, prognostic factors were retrospectively examined and patients who received adjuvant treatment were not included. Pathological scoring was also performed retrospectively by a single urological pathologist. However, this issue is minimized as the pathologist that performed the scoring did not know the clinical information of the patients. Moreover, some i-Cap scores may have been upgraded secondary to surgical removal and/or iatrogenic disruption of the PC during specimen processing. There may also have been inter-observer variability and institutional bias among the investigators who graded the immunostaining score. Furthermore, there were only five cases of i-Cap 0 in the present study. In our other study (unpublished data) of only NSS, it was revealed that ccRCC did not form a PC in some cases (3 out of 11 cases) when the tumor size was <2 cm. The majority of the cases in the present study were nephrectomies, and there were few cases <4 cm that were eligible for NSS, which may be one of the reasons why only five cases of i-Cap 0 were identified. Of the 39 patients in which postoperative metastasis was observed, 14 patients underwent resection of the metastasis. Although it would have been best to evaluate the PCs in the metastatic lesions of all patients, there were cases in which drug therapy was preferred. A feature of the present study is that by using a rat model, the genetic background and tumor background are uniform; therefore, it is possible to

identify a group of genes that are likely to have some significance with a limited number of samples. Subsequently, the genes identified using the rat model were assessed in human samples. However, in the rat model of ccRCC, the expression levels of *ENG* increased as i-Cap score increased, but the opposite result was obtained in human specimens. It was hypothesized that this may be due to species differences or simply due to the smaller numbers assessed in the rat model. Additionally, in the animal model, the kidneys were fixed in formalin immediately after removal so that the gap between the tumor and normal renal tissue could be observed; therefore, another limitation is that it was not possible to remove only the tumor or measure the tumor weight.

In conclusion, the present study investigated the formation and destruction of PCs in ccRCC. PCs were formed by physical compression and tended to collapse as the tumor became malignant. It was revealed that tumor invasion into the PC, that is, disruption of the PC, can be a prognostic factor in ccRCC. Furthermore, PC breakdown was accompanied by degradation of the extracellular matrix by MMP-7, reconstitution by COL4, decreased angiogenesis and infiltration of immune cells.

**Acknowledgements**

Not applicable.

**Funding**

No funding was received.

**Availability of data and materials**

The PCR array data generated in the present study may be found in the NCBI Gene Expression Omnibus (42) under accession numbers GSE255816, GSE255820 and GSE255822 or at the following URLs: https://www.ncbi.nlm.nih.gov/geo/query/acc.cgi?acc=GSE255816, https://www.ncbi.nlm.nih.gov/geo/query/acc.cgi?acc=GSE255820 and https://www.ncbi.nlm.nih.gov/geo/query/acc.cgi?acc=GSE255822. The other data generated in the present study may be requested from the corresponding author.

**Authors' contributions**

TS, MM and KF contributed to the design of the study and writing of the manuscript. KoI, SO, TF, YI, KaI, CO and TM conducted the molecular biology studies. TS and NT performed the statistical tests. FM and MT contributed to the acquisition of data and confirm the authenticity of all the raw data. MM, NT and KF assisted with the writing of the manuscript. All authors read and approved the final manuscript.

**Ethics approval and consent to participate**

The Ethics Committee of Nara Medical University approved this protocol (approval no. NMU-1256). All subjects gave their written informed consent for inclusion before they participated in the study. The institutional animal care and use committee of Nara Medical University approved the animal study protocol (project identification code: 12211).

**Patient consent for publication**

Not applicable.

**Competing interests**

All authors confirm that they have no competing interests.

**References**

1. World Health Organization (WHO): International Agency for Research on Cancer. WHO, Geneva, 2020.
2. Pickhardt PJ, Lonergan GJ, Davis CJ Jr, Kashitani N and Wagner BJ: From the archives of the AFIP. Infiltrative renal lesions: Radiologic-pathologic correlation. Armed forces institute of pathology. Radiographics 20: 215-243, 2000.
3. Minervini A, Carini M, Uzzo RG, Campi R, Smaldone MC and Kutikov A: Standardized reporting of resection technique during nephron-sparing surgery: The surface-intermediate-base margin score. Eur Urol 66: 803-805, 2014.
4. Wang L, Feng J, Alvarez H, Snarskis C, Gupta G and Picken MM: Critical histologic appraisal of the pseudocapsule of small renal tumors. Virchows Arch 467: 311-317, 2015.
5. Minervini A, di Cristofano C, Lapini A, Marchi M, Lanzi F, Giubilei G, Tosi N, Tuccio A, Mancini M, della Rocca C, *et al*: Histopathologic analysis of peritumoral pseudocapsule and surgical margin status after tumor enucleation for renal cell carcinoma. Eur Urol 55: 1410-1418, 2009.
6. Azhar RA, de Castro Abreu AL, Broxham E, Sherrod A, Ma Y, Cai J, Gill TS, Desai M and Gill IS: Histological analysis of the kidney tumor-parenchyma interface. J Urol 193: 415-422, 2015.
7. Cho S, Lee JH, Jeon SH, Park J, Lee SH, Kim CH, Sung JY, Kim JH, Pyun JH, Lee JG, *et al*: A prospective, multicenter analysis of pseudocapsule characteristics: Do all stages of renal cell carcinoma have complete pseudocapsules? Urol Oncol 35: 370-378, 2017.
8. Kryvenko ON: Characteristics of the peritumoral pseudocapsule vary predictably with histologic subtype of T1 renal neoplasms. Jacob JM, Williamson SR, Gondim DD, Leese JA, Terry C, Grignon DJ, Boris RS.Urology. November 2015;86(5):956-961. Urol Oncol 35: 453-454, 2017.
9. Mantoan Padilha M, Billis A, Allende D, Zhou M and Magi-Galluzzi C: Metanephric adenoma and solid variant of papillary renal cell carcinoma: Common and distinctive features. Histopathology 62: 941-953, 2013.
10. Kryvenko ON, Haley SL, Smith SC, Shen SS, Paluru S, Gupta NS, Jorda M, Epstein JI, Amin MB and Truong LD: Haemangiomas in kidneys with end-stage renal disease: A novel clinicopathological association. Histopathology 65: 309-318, 2014.
11. Cho HJ, Kim SJ, Ha US, Hong SH, Kim JC, Choi YJ and Hwang TK: Prognostic value of capsular invasion for localized clear-cell renal cell carcinoma. Eur Urol 56: 1006-1012, 2009.
12. Snarskis C, Calaway AC, Wang L, Gondim D, Hughes I, Idrees MT, Kliethermes S, Maniar V, Picken MM, Boris RS and Gupta GN: Standardized reporting of microscopic renal tumor margins: introduction of the renal tumor capsule invasion scoring system. J Urol 197: 23-30, 2017.
13. Brierley J, Gospodarowicz MK and Wittekind C: TNM classification of malignant tumours. Eigth edition, Wiley Blackwell/John Wiley & Sons, Inc. Chichester, UK, pp 199-201, 2017.
14. Fuhrman SA, Lasky LC and Limas C: Prognostic significance of morphologic parameters in renal cell carcinoma. Am J Surg Pathol 6: 655-663, 1982.
15. Toyokuni S, Uchida K, Okamoto K, Hattori-Nakakuki Y, Hiai H and Stadtman ER: Formation of 4-hydroxy-2-nonenal-modified proteins in the renal proximal tubules of rats treated with a renal carcinogen, ferric nitrilotriacetate. Proc Natl Acad Sci USA 91: 2616-2620, 1994.
16. Vargas-Olvera CY, Sánchez-González DJ, Solano JD, Aguilar-Alonso FA, Montalvo-Muñoz F, Martínez-Martínez CM, Medina-Campos ON and Ibarra-Rubio ME: Characterization of N-diethylnitrosamine-initiated and ferric nitrilotriacetate-promoted renal cell carcinoma experimental model and effect of a tamarind seed extract against acute nephrotoxicity and carcinogenesis. Mol Cell Biochem 369: 105-117, 2012.

17. National Research Council: Guide for the care and use of laboratory animals: Eighth edition. The National Academies Press, Washington, DC, USA, pp 11-18, 2011.
18. Miyake M, Tanaka N, Hori S, Ohnishi S, Takahashi H, Fujii T, Owari T, Ohnishi K, Iida K, Morizawa Y, *et al*: Dual benefit of supplementary oral 5-aminolevulinic acid to pelvic radiotherapy in a syngenic prostate cancer model. Prostate 79: 340-351, 2019.
19. Vandesompele J, De Preter K, Pattyn F, Poppe B, Van Roy N, De Paepe A and Speleman F: Accurate normalization of real-time quantitative RT-PCR data by geometric averaging of multiple internal control genes. Genome Biol 3: research0034.0031, 2002.
20. Livak KJ and Schmittgen TD: Analysis of relative gene expression data using real-time quantitative PCR and the 2(-Delta Delta C(T)) method. Methods 25: 402-408, 2001.
21. Allred DC, Harvey JM, Berardo M and Clark GM: Prognostic and predictive factors in breast cancer by immunohistochemical analysis. Mod Pathol 11: 155-168, 1998.
22. Butcher DT, Alliston T and Weaver VM: A tense situation: Forcing tumour progression. Nat Rev Cancer 9: 108-122, 2009.
23. Handorf AM, Zhou Y, Halanski MA and Li WJ: Tissue stiffness dictates development, homeostasis, and disease progression. Organogenesis 11: 1-15, 2015.
24. Fujimoto N, Sugita A, Terasawa Y and Kato M: Observations on the growth rate of renal cell carcinoma. Int J Urol 2: 71-76, 1995.
25. Oda T, Miyao N, Takahashi A, Yanase M, Masumori N, Itoh N, Tamakawa M and Tsukamoto T: Growth rates of primary and metastatic lesions of renal cell carcinoma. Int J Urol 8: 473-477, 2001.
26. Lohi J, Korhonen M, Leivo I, Kangas L, Tani T, Kalluri R, Miner JH, Lehto VP and Virtanen I: Expression of type IV collagen alpha1(IV)-alpha6(IV) polypeptides in normal and developing human kidney and in renal cell carcinomas and oncocytomas. Int J Cancer 72: 43-49, 1997.
27. Best SL, Liu Y, Keikhosravi A, Drifka CR, Woo KM, Mehta GS, Altwegg M, Thimm TN, Houlihan M, Bredfeldt JS, *et al*: Collagen organization of renal cell carcinoma differs between low and high grade tumors. BMC Cancer 19: 490, 2019.
28. Provenzano PP, Eliceiri KW, Campbell JM, Inman DR, White JG and Keely PJ: Collagen reorganization at the tumor-stromal interface facilitates local invasion. BMC Med 4: 38, 2006.
29. Gu ZD, Li JY, Li M, Gu J, Shi XT, Ke Y and Chen KN: Matrix metalloproteinases expression correlates with survival in patients with esophageal squamous cell carcinoma. Am J Gastroenterol 100: 1835-1843, 2005.
30. Miyata Y, Iwata T, Ohba K, Kanda S, Nishikido M and Kanetake H: Expression of matrix metalloproteinase-7 on cancer cells and tissue endothelial cells in renal cell carcinoma: Prognostic implications and clinical significance for invasion and metastasis. Clin Cancer Res 12: 6998-7003, 2006.
31. Ogawa M, Ikeuchi K, Watanabe M, Etoh K, Kobayashi T, Takao Y, Anazawa S and Yamazaki Y: Expression of matrix metalloproteinase 7, laminin and type IV collagen-associated liver metastasis in human colorectal cancer: Immunohistochemical approach. Hepatogastroenterology 52: 875-880, 2005.
32. Liao HY, Da CM, Liao B and Zhang HH: Roles of matrix metalloproteinase-7 (MMP-7) in cancer. Clin Biochem 92: 9-18, 2021.
33. Ishikawa T, Kimura Y, Hirano H and Higashi S: Matrix metalloproteinase-7 induces homotypic tumor cell aggregation via proteolytic cleavage of the membrane-bound Kunitz-type inhibitor HAI-1. J Biol Chem 292: 20769-20784, 2017.
34. Motzer RJ, Banchereau R, Hamidi H, Powles T, McDermott D, Atkins MB, Escudier B, Liu LF, Leng N, Abbas AR, *et al*: Molecular subsets in renal cancer determine outcome to checkpoint and angiogenesis blockade. Cancer Cell 38: 803-817.e4, 2020.
35. Ohe C, Yoshida T, Amin MB, Atsumi N, Ikeda J, Saiga K, Noda Y, Yasukochi Y, Ohashi R, Ohsugi H, *et al*: Development and validation of a vascularity-based architectural classification for clear cell renal cell carcinoma: correlation with conventional pathological prognostic factors, gene expression patterns, and clinical outcomes. Mod Pathol 35: 816-824, 2022.
36. Cioca A, Muntean D and Bungardean C: CD105 as a tool for assessing microvessel density in renal cell carcinoma. Indian J Pathol Microbiol 62: 239-243, 2019.
37. Rooney MS, Shukla SA, Wu CJ, Getz G and Hacohen N: Molecular and genetic properties of tumors associated with local immune cytolytic activity. Cell 160: 48-61, 2015.
38. Şenbabaoğlu Y, Gejman RS, Winer AG, Liu M, Van Allen EM, de Velasco G, Miao D, Ostrovnaya I, Drill E, Luna A, *et al*: Tumor immune microenvironment characterization in clear cell renal cell carcinoma identifies prognostic and immunotherapeutically relevant messenger RNA signatures. Genome Biol 17: 231, 2016.
39. Galon J, Pagès F, Marincola FM, Angell HK, Thurin M, Lugli A, Zlobec I, Berger A, Bifulco C, Botti G, *et al*: Cancer classification using the immunoscore: A worldwide task force. J Transl Med 10: 205, 2012.
40. Pagès F, Mlecnik B, Marliot F, Bindea G, Ou FS, Bifulco C, Lugli A, Zlobec I, Rau TT, Berger MD, *et al*: International validation of the consensus immunoscore for the classification of colon cancer: A prognostic and accuracy study. Lancet 391: 2128-2139, 2018.
41. Fridman WH, Zitvogel L, Sautès-Fridman C and Kroemer G: The immune contexture in cancer prognosis and treatment. Nat Rev Clin Oncol 14: 717-734, 2017.
42. Edgar R, Domrachev M and Lash AE: Gene expression omnibus: NCBI gene expression and hybridization array data repository. Nucleic Acids Res 30: 207-210, 2002.